Gamma-ray multiplicity distribution associated with massive transfer

T. Inamura
Cyclotron Laboratory, RIKEN (The Institute of Physical and Chemical Research), Wako-shi, Saitama 351-01, Japan and Cyclotron Institute, Texas A&M University, College Station, Texas 77843

A. C. Kahler,* D. R. Zolnowski,† U. Garg,‡ and T. T. Sugihara§
Cyclotron Institute, Texas A&M University, College Station, Texas 77843

M. Wakai
Department of Physics, Osaka University, Toyonaka, Osaka 560, Japan
(Received 15 July 1985)

The first three moments of the γ-ray multiplicity distribution were measured for individual αxn exit channels of the reactions 85-MeV $^{12}C+^{154}Sm$, 109-MeV $^{12}C+^{154}Sm$, and 115-MeV $^{14}N+^{159}Tb$, in which massive transfer had been studied previously. The average γ multiplicity (first moment) was found to be almost constant, independent of yrast spin for fast α-particle emission, while it increases with yrast spin for slow α-particle emission as is common in complete fusion. The variance (second moment) is also independent of yrast spin. For fast α-particle emission, the average γ multiplicity decreases monotonically with increasing α-particle energy, and simultaneously the skewness (third moment) tends to be positive. This indicates that massive transfer accompanied by fast α-particle emission is similar to a quasielastic process in heavy-ion reactions. A statistical model calculation has been made to study the dependence of the γ-ray multiplicity distribution on angular momentum and excitation energy. The results are consistent with the experimental data. It is found that the sign of skewness depends on the widths of angular-momentum and excitation-energy distributions.

I. INTRODUCTION

It was in 1961 that Britt and Quinton suggested the possibility of what is now called direct breakup fusion in their pioneering work on light charged-particle emission in heavy-ion induced reactions.[1] Experimentally, however, Inamura *et al.*[2] first demonstrated this possibility: They clearly observed that when fast α particles were emitted in the 95-MeV $^{14}N+^{159}Tb$ reaction the massive fragment ^{10}B of the projectile was transferred to the target nucleus to fuse. Furthermore, they noted the lack of sidefeeding at low spins ($\lesssim 10\hbar$) in the residual nucleus produced via this new reaction and argued the existence of a localized window in l space as a result of a peripheral collision. Since then, systematic studies of reactions of this type have been carried out at Texas A&M (Refs. 3 and 4) and related work has been reported by groups at Groningen,[5,6] Oak Ridge,[7–9] and Orsay.[10]

By "massive transfer" we mean those heavy-ion induced reactions in which a relatively heavy part of the projectile is transferred to the target nucleus in a peripheral reaction. The resulting compound system of massive fragment plus target deexcites by evaporation of particles and by γ decay. The remaining light fragment from the projectile (typically a proton or an α particle) is observed as a forward-peaked, energetic, spectator particle. Massive transfer appears to be a universal process associated with heavy-ion reactions.[11] But the underlying reaction mechanism is not yet clear. These reactions have also been referred to as "incomplete fusion." The possibility of incomplete fusion in heavy-ion reactions was first pointed out by Lefort,[12] who suggested that it might be a sort of deep-inelastic process.

Several theoretical approaches have been made to describe the mechanism of massive transfer (or incomplete fusion) reactions by taking into account the direct interaction between projectile and target nuclei.[13–17] Kishimoto-Kubo,[13] Udagawa-Tamura,[14] and Bunakov *et al.*[15] employed basically a DWBA approach. Others attempted to explain fast light-particle emission in general. Wilczynski *et al.*[17] describe all types of incomplete fusion reactions as binary l-matched reactions and include complete fusion on the same footing. All theories require localization in l space.

In order to get more direct information on angular momentum than the γ-ray intensity pattern provides, Inamura *et al.*[18] and Geoffroy *et al.*[7] measured average γ-ray multiplicities for these reactions, selecting individual exit channels; the latter group also measured the second moments from which the width of angular momentum distribution might be estimated. (They measured the first three moments for all γ rays but not for individual exit channels.) All of their results are consistent with the previous conjecture that there exists a localized window in angular momentum, and Geoffroy *et al.*[7] have reported that their results are in agreement with predictions of the model of successive l windows.[5] However, the reason why and the extent to which the l space is localized is not yet entirely convincing. It is of vital importance to have more information on this problem, especially for individual exit

channels of the reaction in question.

In the present experiments the γ-ray multiplicity distributions were measured for αxn channels of the $^{12}C + ^{154}Sm$ and $^{14}N + ^{159}Tb$ systems in which massive-transfer reactions had been studied previously.[3] The first three moments were extracted for each reaction channel and studied not only as a function of α particle energy but also as a function of yrast spin. To examine the dependence of the γ-ray multiplicity distribution on angular momentum and excitation energy, a statistical model calculation was made for complete fusion and massive transfer. The sign of the third moment (skewness) is closely related to the widths of angular-momentum and excitation-energy distributions. We shall point out an interesting similarity between massive transfer and quasi-elastic scattering. Some aspects of the present study have already been discussed in Refs. 11, and 19–21.

II. EXPERIMENTAL PROCEDURE

Self-supporting metallic targets of ^{154}Sm and ^{159}Tb were used in the present experiments. The ^{154}Sm target was 98.7% enriched and 2 mg/cm^2 in thickness. The ^{159}Tb target was 2.5 mg/cm^2 in thickness. ^{154}Sm was bombarded with 85- and 109-MeV ^{12}C beams from the Texas A&M University cyclotron, and ^{159}Tb with a 115-MeV ^{14}N beam.

The $^{12}C + ^{154}Sm$ reaction mainly leads to αxn products $^{162-x}Dy$ and $2\alpha xn$ products $^{158-x}Gd$, and the $^{14}N + ^{159}Tb$ reaction leads to αxn products $^{169-x}Yb$. Gamma-ray multiplicities for these reaction products were measured using a multidetector system. This system consists of eight 7.5-cm-diam by 7.5-cm-long NaI(Tl) detectors, four of which are above and four below the reaction plane in hemispherical arrays. Each detector makes an angle of 55° to the beam direction to minimize the effect of γ-ray angular distributions.

Lead (2.5 cm minimum) was used to shield the individual detectors from each other within each hemisphere. The detectors were placed 12 cm from the target, and Al (7.75 mm thick) and Cu (5.0 mm thick) disks were used to attenuate low-energy γ rays. The absolute detection efficiency Ω of each detector was 0.012 for γ rays in the energy range 0.2–5 MeV within 10% accuracy.

Charged particles emitted were detected with $\Delta E - E$ Si detector stacks; usually two sets of detector stacks were placed symmetrically at 20° to the beam. Detector slits with a 1 cm^2 opening located about 9.5 cm from the target permitted a nominal angular definition of ±3°. Thin Al foils were placed at the slits to prevent scattered beams from reaching the detector. A coaxial Ge(Li) detector was placed at 90° to the beam and about 6 cm from the target. Ge(Li) spectra were registered in coincidence with emitted α particles and with NaI detectors. Data were recorded event by event on magnetic tapes, which were replayed on a VAX-11/780 computer. Yields of discrete γ-ray lines were measured as a function of the "fold" number, i.e., the number of NaI detectors fired. An example of γ-ray spectra observed is presented in Fig. 1.

To deduce the first three moments of the γ-ray multiplicity distribution, yields of discrete γ-ray lines coincident with α particles and NaI detectors were analyzed using a nonlinear method.[22] Although they are much less sensitive to neutrons, the NaI detectors may be fired by neutrons, resulting in some false events. To correct for this effect, we assumed an effective neutron detection efficiency $\Omega_\nu = 0.0012$. This assumption is consistent with results reported by Sarantites *et al.*[23]

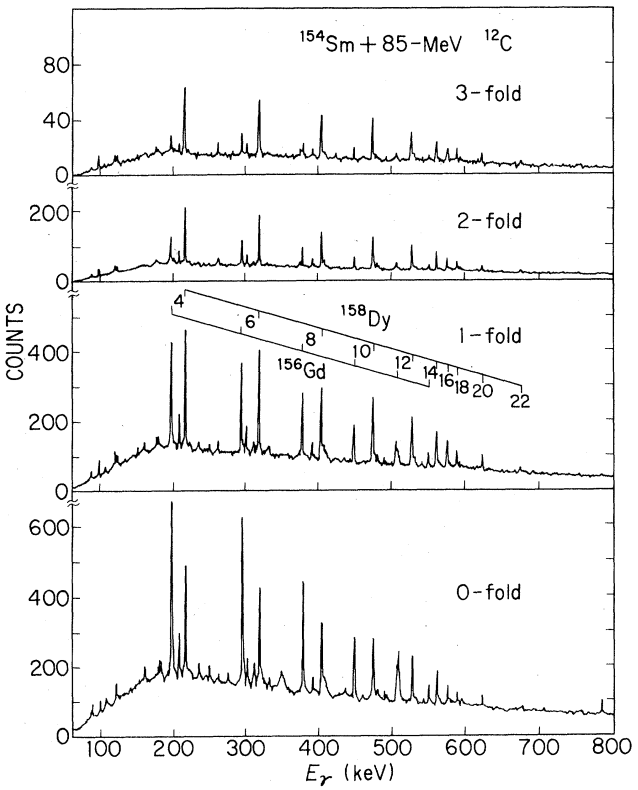

FIG. 1. Gamma spectra coincident with α particles and 0–3 NaI(Tl) detectors following the $^{12}C + ^{154}Sm$ reaction at 85 MeV.

One can easily incorporate this correction into the formalism given in Ref. 22: a generating function G_n, i.e., the probability of observing no coincidences in $(N-n)$ detectors is written as

$$\langle G_n \rangle = \langle [1-(N-n)\Omega]^M \cdot [1-(N-n)\Omega_\nu]^{M_\nu} \rangle , \quad (1)$$

where M_ν is the number of neutrons emitted. M_ν is known exactly if a discrete gating γ ray is given.

We also tried to see the effect of γ-ray summing in a Ge(Li) detector, as discussed by Sujkowksi and van der Werf.[24] In general, the convergence became worse with this correction than without it. This may be a worthwhile study in itself. But here we shall not go into this problem because in any case the summing correction is at most ten per cent in the present case, so that the γ multiplicity extracted without this correction does not cause any serious problems for the present purpose.

III. EXPERIMENTAL RESULTS

The first three moments of the γ-ray multiplicity distribution were extracted for yrast transitions in $^{158-x}Gd$ and

$^{162-x}$Dy products from the $^{12}C + ^{154}Sm$ reaction and in $^{169-x}$Yb products from the $^{14}N + ^{159}Tb$ reaction. These moments have been converted into shape parameters, i.e., the average multiplicity $\langle M \rangle$, the standard deviation of the distribution σ_M, and the skewness s_M, as described in Sec. IV. The shape parameters obtained for α-particle energy $E_\alpha \geq 20$ MeV in the laboratory system are summarized in Table I, where the gating transition is the $4^+ \rightarrow 2^+$ transition in even residues and the $\frac{17}{2}^+ \rightarrow \frac{13}{2}^+$ transition in odd residues which normally gave the most intense γ-ray yields. Those values of $\langle M \rangle$ are somewhat smaller and more precisely determined than the preliminary results reported in Ref. 11. It should be pointed out that the sign of s_M is likely to be positive when the number of neutrons in the αxn channel is relatively small or in case of the $2\alpha xn$ channel. In the $^{12}C + ^{154}Sm$ reaction at 109 MeV, the $2\alpha xn$ channel is somewhat competing with the αxn channel, and therefore the shape parameters are presented for $2\alpha xn$ as well as for αxn channels.

Shape parameters versus yrast spin are compared for various αxn channels in Figs. 2–4. As is seen in Fig. 2, in the case of the $^{159}Tb(^{14}N,\alpha xn)^{169-x}Yb$ reactions at 115 MeV, $\langle M \rangle$ appears to increase with increasing spin when the number of neutrons emitted is large (e.g., $x=6$), while it appears independent of spin when the number of neutrons is small. The standard deviation σ_M appears to decrease with increasing spin when the number of neutrons is large, and likely to be independent of spin when the number of neutrons is small. There seems to be the same tendency in the case of the $^{154}Sm(^{12}C,\alpha xn)^{162-x}Dy$ reactions at 109 MeV. (See Fig. 4.) In Fig. 5 the same plots are made for the $^{154}Sm(^{12}C,2\alpha xn)^{158-x}Gd$ reactions at 109 MeV for comparison.

Figure 6 shows plots of $\langle M \rangle$ vs yrast spin which were observed for different energy bins of α particles emitted in the $^{159}Tb(^{14}N,\alpha 5n)^{164}Yb$ reaction at 115 MeV. When gated by low-energy α particles ($E_\alpha < 30$ MeV), $\langle M \rangle$ tends to increase with spin. This energy range corresponds to that of α particles evaporated from the fully equilibrated system of $^{14}N + ^{159}Tb$. For fast α particles ($E_\alpha > 30$ MeV) $\langle M \rangle$ vs spin is flattened. As shown in Fig. 2, $\langle M \rangle$ is almost independent of spin except for the case of ^{163}Yb when all α particles are included. This is consistent with the weighted average of $\langle M \rangle$ values obtained for α-particle energy bins.

Shape parameters obtained for individual reaction channels are shown in Fig. 7 as a function of α-particle energy E_α. A general tendency that $\langle M \rangle$ decreases monotonically with increasing E_α ($E_\alpha \gtrsim 30$ MeV) is seen; in the relatively low energy region, i.e., the region of α-particle evaporation from a fully equilibrated system, $\langle M \rangle$ seems to be saturated. There is another remarkable behavior in the tendency of s_M: The sign of s_M tends to be positive for fast α-particle emission. In the region of slow α particles s_M is likely to be negative as always expected in the case of complete fusion evaporation. (See Secs. IV and V.)

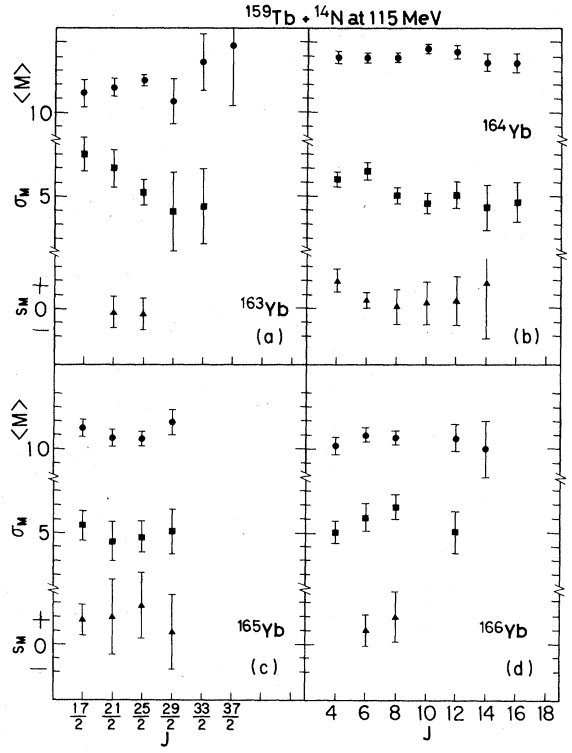

FIG. 2. Shape parameters of the γ-ray multiplicity distribution versus yrast spin observed for the $^{159}Tb(^{14}N,\alpha xn)^{169-x}Yb$ reactions at 115 MeV.

TABLE I. Shape parameters describing γ-ray multiplicity distributions for the $^{12}C + ^{154}Sm$ and $^{14}N + ^{159}Tb$ reactions. Numbers in parentheses indicate the statistical uncertainties in the least significant figure.

Reaction	85-MeV $^{12}C + ^{154}Sm$			109-MeV $^{12}C + ^{154}Sm$			115-MeV $^{14}N + ^{159}Tb$		
	$\langle M \rangle$	σ_M	s_M	$\langle M \rangle$	σ_M	s_M	$\langle M \rangle$	σ_M	s_M
α3n							11.0(5)	6.1(10)	+ 1.0(11)
α4n	12.1(2)	4.5(3)	+ 1.7(4)	14.7(10)	6.2(17)	+ 2.4(18)	11.5(6)	5.6(10)	+ 1.8(11)
α5n				11.8(3)	4.8(5)	+ 0.3(5)	13.9(3)	6.2(5)	+ 1.9(7)
α6n				12.1(3)	4.1(9)	− 1.7(22)	11.8(6)	7.0(12)	− 0.3(11)
2α2n	6.6(1)	4.2(2)	+ 2.6(3)	7.6(3)	4.7(9)	+ 1.0(5)			
2α3n				8.3(10)	5.1(16)	+ 0.5(13)			
2α4n				8.6(3)	5.7(3)	+ 0.6(3)			

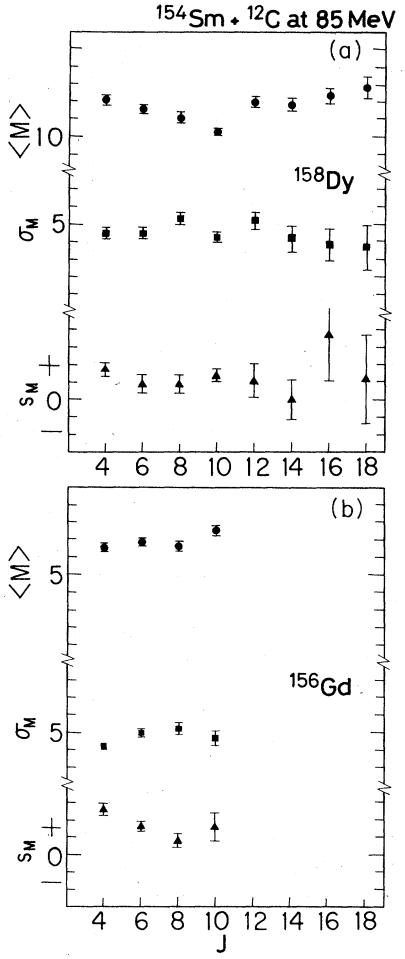

FIG. 3. Shape parameters of the γ-ray multiplicity distribution versus yrast spin observed for (a) ^{154}Sm(^{12}C,α4n)^{158}Dy, and (b) ^{154}Sm(^{12}C,2α2n)^{156}Gd reactions at 85 MeV.

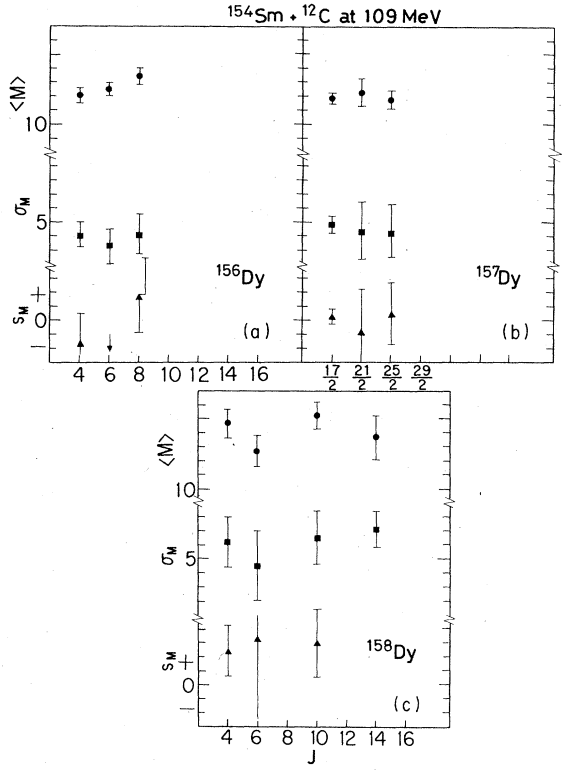

FIG. 4. Shape parameters of the γ-ray multiplicity distribution versus yrast spin observed for the ^{154}Sm(^{12}C,αxn)$^{162-x}$Dy reactions at 109 MeV.

IV. STATISTICAL MODEL CALCULATION OF γ-RAY MULTIPLICITY DISTRIBUTION

We have carried out a statistical model calculation to study the dependence of the γ-ray multiplicity distribution on spin J and excitation energy E. The first three moments of the distribution are defined as

$$\mu_n = \frac{1}{N}\sum_{i=1}^{N}(M_i - \overline{M})^n , \tag{2}$$

M_i being the number of γ transitions at the ith trial. (Each trial is randomly generated in the calculation.) By taking the central moments, i.e., $\overline{M} = \langle M \rangle$ where $\langle M \rangle$ is the arithmetic mean value (from now on the average multiplicity), the shape parameters of the distribution have been estimated as follows: the standard deviation

$$\sigma_M = \sqrt{\mu_2} , \tag{3}$$

and the skewness

$$s_M = \frac{\mu_3}{\sigma_M^3} . \tag{4}$$

If $s_M = 0$, i.e., $\mu_3 = 0$, M_i distributes symmetrically about the average value $\langle M \rangle$. A part of this computational study has been reported in Ref. 19.

A. Method of calculation

Computation was made by combining the second part of the Monte Carlo treatment code ICARUS (Region II) (Ref. 25) and the code GROGI2.[26] The ICARUS code has successfully been applied to extract the γ-ray multiplicity distribution and the population of yrast states in the case of complete fusion reactions.[25] For the present purpose the time-consuming first part of ICARUS (Region I), which treats the multiparticle evaporation process, was replaced by GROGI2 because it was found that when it was normalized, the entry-state population $P(E,J)$ produced by the ICARUS (Region I) was not substantially different from the one obtained with GROGI2. In the GROGI2 computation α particles were treated as being emitted first followed by successive neutron evaporation. Although it is not experimentally established yet, nonstatistical fast neutron emission is unlikely in the massive-transfer (or incomplete fusion) reaction accompanying energetic α-particle emission.[2-10]

There are two basic quantities to be chosen in the code GROGI2:[26] the level density and the γ-decay width. We have tested how the entry-state population $P(E,J)$ would change with these quantities, changing parameters inherent in them.[26]

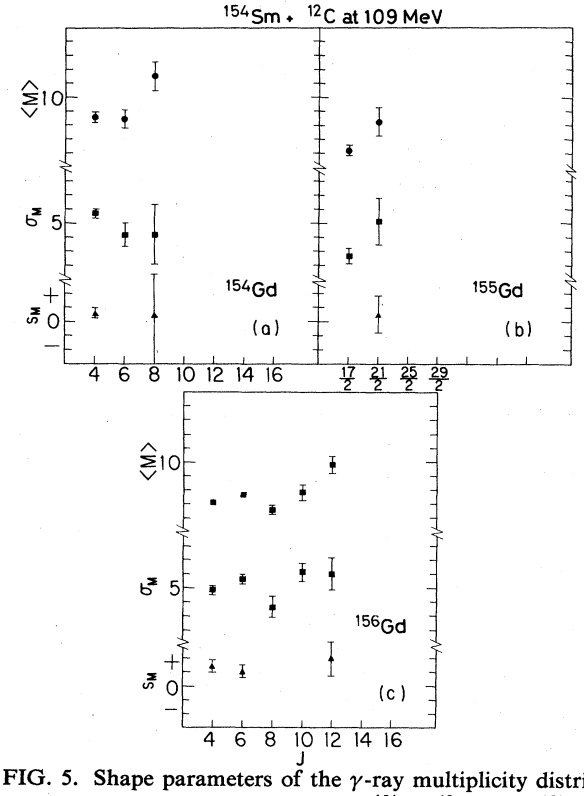

FIG. 5. Shape parameters of the γ-ray multiplicity distribution versus yrast spin observed for the ^{154}Sm(^{12}C,$2\alpha x$n)$^{158-x}$Gd reactions at 109 MeV.

We found that neither the γ-ray multiplicity distribution nor the shape of $P(E,J)$ was sensitive to their choices. For instance, the Sperber correction,[27] which is a correction for the γ-decay width, changed the production

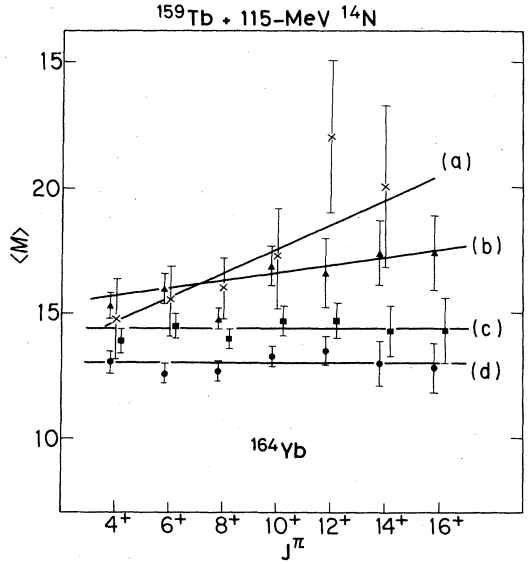

FIG. 6. $\langle M \rangle$ vs yrast spin observed for the energy bin of α particles emitted in the ^{159}Tb(^{14}N,α5n)^{164}Yb reaction at 115 MeV: (a) $22 \leqq E_\alpha \leqq 25$, (b) $25 \leqq E_\alpha \leqq 30$, (c) $30 \leqq E_\alpha \leqq 35$, (d) $E_\alpha > 35$ MeV in the laboratory system. Solid lines are drawn to guide the eye.

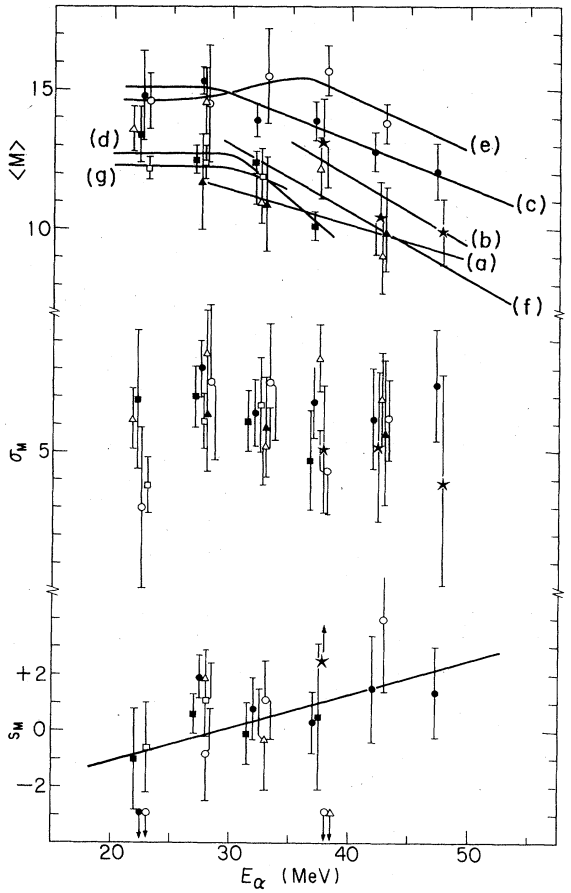

FIG. 7. Shape parameters of the γ-ray multiplicity distribution as a function of α-particle energy E_α in the laboratory system for individual reaction channels. Closed points indicate those of the ^{159}Tb(^{14}N,αxn)$^{169-x}$Yb reactions at 115 MeV: symbol ▲ and (a) are for $x=3$; ★ and (b) for $x=4$; ● and (c) for $x=5$; and ■ and (d) for $x=6$. Open points indicate those of the ^{154}Sm(^{12}C,αxn)$^{162-x}$Dy reactions at 109 MeV: symbol ○ and (e) are for $x=4$; △ and (f) for $x=5$; and □ and (g) for $x=6$. Flags indicate statistical errors. Solid lines are drawn to guide the eye.

cross section for residual nuclei most significantly, but the shape of $P(E,J)$ at later neutron emission steps (4—5 neutron evaporation in the present calculation) was almost the same with that obtained with the standard recipe.[26] Therefore, we used the standard recipe throughout the present study.

There are two basic quantities also in the code ICARUS (Region II): the level density and the ratio of γ transition strengths C_{E1}:C_{M1}:C_{E2}:$C_{E2}^{\rm coll}$. We adopted the ratio of 500:25:1:200 that was originally proposed for the case of ^{162}Er.[25]

It is known that the γ-deexcitation pattern is mainly affected by the ratio C_{E1}:$C_{E2}^{\rm coll}$.[25] We checked the dependence of γ-ray multiplicity distribution on this ratio, and we found that the values of $\langle M \rangle$ and σ_M were hardly affected, even if the ratio was changed by a factor of 10. Therefore, the ratio, C_{E1}:C_{M1}:C_{E2}:$C_{E2}^{\rm coll}$, we adopted should be good enough for the present purpose because we are concerned with the nuclei in the neighborhood of

^{162}Er. Although the absolute value of s_M is affected apparently by changing the ratio, its sign is not altered. As was briefly mentioned in Ref. 19, this leads to the conclusion that the sign of s_M is determined by the shape of $P(E,J)$, independent of the γ-deexcitation process. (See Sec. IV B.)

For the GROGI2 computation to produce the entry-state population $P(E,J)$ via massive transfer, the input excitation energy ϵ and angular momentum λ distribution in the compound system formed by the massive fragment plus target was assumed to be given by

$$p(\epsilon,\lambda)=N\exp\left[-\frac{1}{2}\left[\frac{\epsilon-\langle\epsilon\rangle}{\sigma_\epsilon}\right]^2\right]\times\exp\left[-\frac{1}{2}\left[\frac{\lambda-\langle\lambda\rangle}{\sigma_\lambda}\right]^2\right], \quad (5)$$

where N is a normalization constant, $\langle\epsilon\rangle$ and $\langle\lambda\rangle$ are mean values of ϵ and λ, respectively, and σ indicates a standard deviation. Gaussian forms of ϵ and λ distributions should be reasonably good for the present purpose because our interest is in gross properties of the deexcitation process.

The mean excitation energy $\langle\epsilon\rangle$ is estimated from the relation

$$\langle\epsilon\rangle=E_p-\langle E_\alpha\rangle-S_\alpha+Q\ , \quad (6)$$

where E_p is the kinetic energy of the projectile in the center-of-mass system, S_α the separation energy of an α particle in the projectile, and Q the Q value for fusion of the massive fragment and the target.

In the case of the 115-MeV N + ^{159}Tb reaction, $\langle\epsilon\rangle\approx 64$ MeV at $\langle E_\alpha\rangle\approx 30$ MeV: at this energy of α particles the 5n channel from the remaining compound system ^{10}B + ^{159}Tb is most favored. The standard deviation σ_ϵ was estimated from the experimental E_α spectrum,[11] whose full width at half maximum (FWHM) ΔE_α was about 15 MeV, by assuming $\Delta E_\alpha=2.35\sigma_\epsilon$.

According to Udagawa and Tamura,[14] the centroid of the λ window in the massive-transfer reaction of 115-MeV ^{14}N with ^{159}Tb in which 30-MeV α particles are emitted is $\langle\lambda\rangle=26\hbar$ and the FWHM is $\Delta\lambda=7\hbar$. They also estimate that $d\lambda/dE_\alpha$ is about $-0.3\hbar$ per MeV. Since $\Delta E_\alpha\approx 15$ MeV, $\Delta\lambda$ will be increased by about $5\hbar$ so that $\Delta\lambda\approx 12\hbar$ and σ_λ is estimated by the relation $\Delta\lambda=2.35\sigma_\lambda$.

The calculated $P(E,J)$ distribution for the massive-

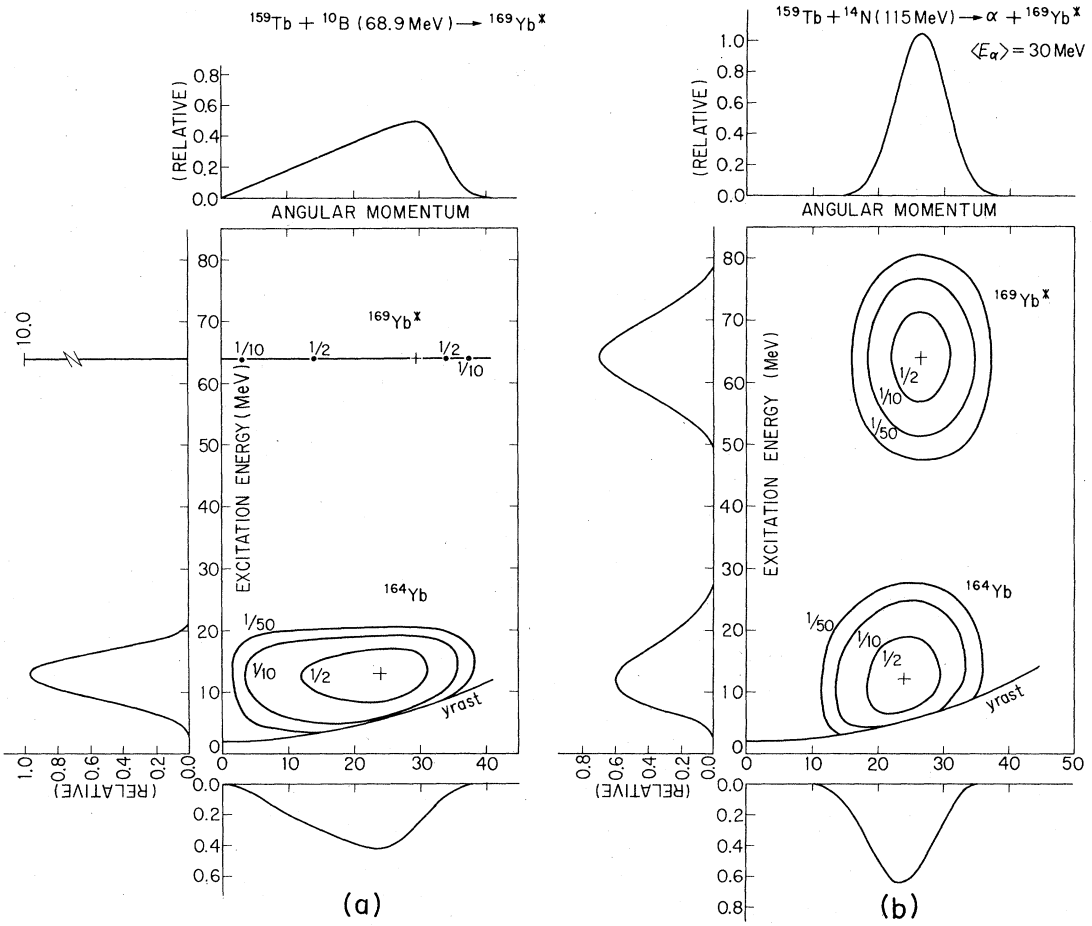

FIG. 8. Comparison of population of excited states via (a) complete fusion and (b) massive transfer. Computation has been made using the computer code GROGI2.[26]

TABLE II. Examples of the statistical model calculation on massive-transfer and complete-fusion reaction products.

Reaction	Exit channel	Product	$\langle M \rangle$	σ_M	s_M
85-MeV $^{12}C + {}^{154}Sm$[a]	α4n	^{158}Dy	11.2	2.3	0.12
109-MeV $^{12}C + {}^{154}Sm$[a]	α4n	^{158}Dy	12.9	2.6	0.07
115-MeV $^{14}N + {}^{159}Tb$[b]	α5n	^{164}Yb	14.6	3.1	0.25
69-MeV $^{10}B + {}^{159}Tb$[c]	5n	^{164}Yb	13.7	3.7	−0.10
115-MeV $^{14}N + {}^{159}Tb$[d]	α5n	^{164}Yb	18.4	4.6	−0.05

[a]Massive transfer. The transferred fragment is ^{8}Be.
[b]Massive transfer. The transferred fragment is ^{10}B.
[c]Fusion. The excitation energy of the system for this ^{10}B energy corresponds to the excitation energy at the most probable energy of α particles emitted in the massive-transfer reaction $^{159}Tb(^{14}N,\alpha 5n)^{164}Yb$ at 115 MeV.
[d]Fusion evaporation.

transfer residue ^{164}Yb is shown in Fig. 8. For comparison, calculation has been made for complete fusion in the 115-MeV $^{14}N + {}^{159}Tb$ and 69-MeV $^{10}B + {}^{159}Tb$ reactions. As is shown in Fig. 8(a), the latter gives about the same excitation in the compound system as the massive transfer ($^{10}B + {}^{159}Tb$) does in the former on the average. However, a significant difference in $P(E,J)$ is seen between complete fusion and massive transfer. The difference becomes much larger in the case of complete fusion of 115-MeV ^{14}N with ^{159}Tb.

For complete fusion, the initial angular momentum distribution $p(\lambda)$ in the compound system was given by

$$p(\lambda)=\frac{2\lambda+1}{1+\exp\left[\dfrac{\lambda-\lambda_c}{\delta}\right]}, \tag{7}$$

where λ_c is the critical angular momentum for fusion that was estimated from a sharp cutoff model described by Lefort and Ngo;[28] and the diffuseness parameter δ was chosen to be $\delta=1.5\hbar$ in this mass region by making an optical model calculation (ABACUS−2).[29]

The shape parameters were calculated for the $4^+\rightarrow 2^+$ transitions in the residual nuclei ^{158}Dy and ^{164}Yb which were produced by the reactions $^{12}C + {}^{154}Sm$ and $^{14}N + {}^{159}Tb$, respectively. The results are summarized in Table II. Although no calculation was made for the massive-transfer reaction in the $^{12}C + {}^{154}Sm$ system by Udagawa and Tamura,[14] we have assumed the same ratio of $\langle\lambda\rangle$ to the critical angular momentum Λ_c for fusion[28] of the massive fragment and target nuclei as that estimated for the 115-MeV $^{14}N + {}^{159}Tb$ reaction, i.e., $\langle\lambda\rangle/\Lambda_c=0.8$, since the breakup-fusion model[14] is expected to give about the same ratio of $\langle\lambda\rangle/\Lambda_c$ for these two systems in which the combination of projectile and target is similar.

The present model calculation accounts well for the γ-ray intensity patterns of yrast transitions observed in massive-transfer reactions. Figure 9 presents a typical ex-

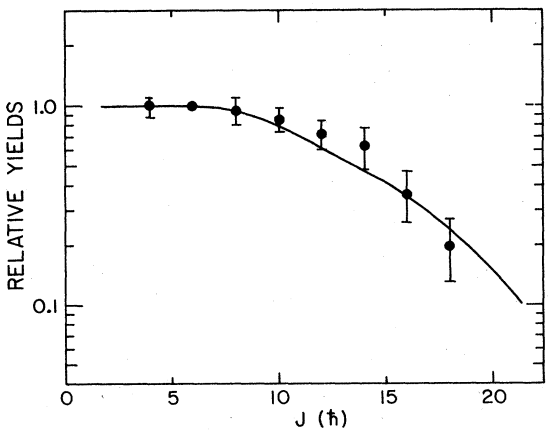

FIG. 9. Intensity of yrast transitions relative to the $6^+\rightarrow 4^+$ transition in ^{164}Yb produced via the massive-transfer reaction $^{159}Tb(^{14}N,\alpha 5n)^{164}Yb$ at 115 MeV. Experimental data are from Ref. 3. Solid curve is the statistical model calculation made at $E_\alpha=30$ MeV.

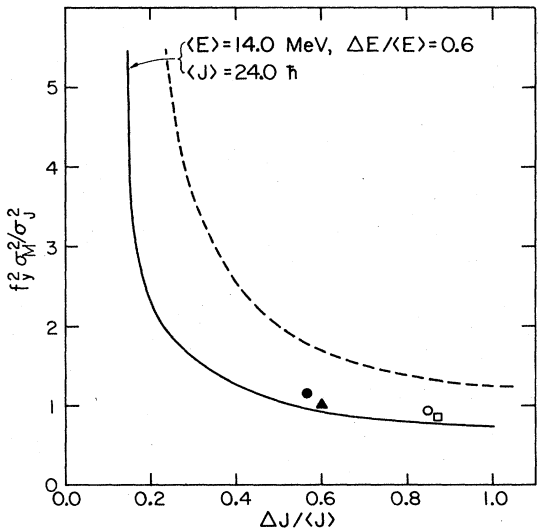

FIG. 10. The ratio $f_y^2\sigma_M^2/\sigma_J^2$ as a function of $\Delta J/\langle J\rangle$. The solid curve is the present statistical calculation. The dotted curve is obtained with a simplified relation of σ_M and σ_J which is given in Ref. 30. Solid and open points represent the ratios calculated for the following massive transfer and fusion reactions: massive transfer, $^{159}Tb(^{14}N,\alpha 5n)^{164}Yb$ at 115 MeV (indicated by ●), and $^{154}Sm(^{12}C,\alpha 4n)^{158}Dy$ at 85 and 109 MeV (▲); fusion, $^{159}Tb(^{10}B,5n)^{164}Yb$ at 69 MeV (○), and $^{159}Tb(^{14}N,\alpha 5n)^{164}Yb$ at 115 MeV (□).

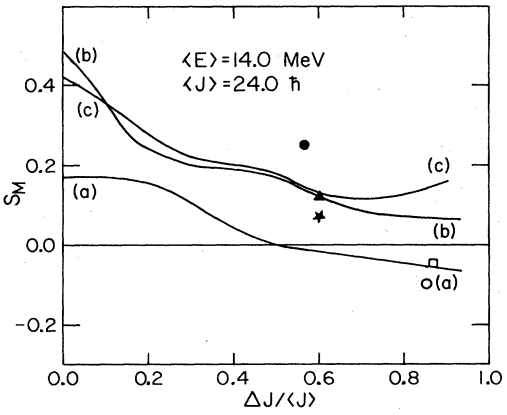

FIG. 11. Dependence of skewness s_M on the entry-state E and J distributions: (a) $\Delta E/\langle E\rangle=0.0$, (b) $\Delta E/\langle E\rangle=0.6$, and (c) $\Delta E/\langle E\rangle=0.9$. Points indicated are the same as in Fig. 10, but the solid star is s_M calculated for the massive transfer ^{154}Sm(^{12}C,α4n)^{158}Dy at 109 MeV. (Cited from Ref. 19.)

ample: 115-MeV ^{14}N + ^{159}Tb, experimental data of which are cited from Ref. 3.

B. Relationship between the γ-ray multiplicity distribution and the entry-state population

To elucidate the relationship between the γ-ray multiplicity distribution and the entry-state population $P(E,J)$, we carried out the ICARUS computation on ^{164}Yb, assuming $P(E,J)=P(E)\cdot P(J)$: $P(E)$ and $P(J)$ are Gaussian as in Eq. (5). Since the code ICARUS takes the yrast line into account,[25] this input assumption is considered reasonably good for the present purpose.

In Fig. 10 the ratio of quantity $f_y^2\sigma_M^2$ to σ_J^2 is plotted as a function of $\Delta J/\langle J\rangle$ where $\Delta J=2.35\sigma_J$ and f_y is the angular momentum carried away by each of yrast transitions (here $f_y=2\hbar$). The solid curve was obtained for $P(E,J)$ with $\langle E\rangle=14$ MeV, $\Delta E/\langle E\rangle=0.6$, and $\langle J\rangle=24\hbar$; ΔE is the FWHM of the E distribution, which is given by ΔE_α, the FWHM of the E_α spectrum. These values are extracted from the entry-state population calculated for the massive-transfer reaction ^{159}Tb(^{14}N,α5n)^{164}Yb at 115 MeV. (See Sec. IV A.) The ratio was found to be within 10% of the solid curve for a wide range in E-J space, $\langle E\rangle=12$–20 MeV, $\langle J\rangle=18\hbar$–$30\hbar$ and various values of $\Delta E/\langle E\rangle$. It should also be stated that σ_M was almost independent of ΔE.

The dotted curve presents the same ratio that was calculated using a simplified relationship[30]

$$\sigma_M^2=\frac{\sigma_J^2}{f_y^2}+\left[\frac{f_s-f_y}{f_y}\right]^2\sigma_s^2\,, \tag{8}$$

where σ_s is the standard deviation of the statistical γ-ray multiplicity distribution, and f_s is the angular momentum carried away by each of the statistical γ transitions; we used $\sigma_s^2=10$, and $f_s=0.4$ according to Ref. 30. As is seen from Fig. 10, there is a large difference between the two curves. This is quite natural because the present statistical calculation (solid curve) automatically includes the effect of the covariance term between σ_M and σ_s while Eq. (8) does not. One has to bear in mind that extreme care should be taken in the use of such a simplified relation as Eq. (8) to extract σ_J from σ_M. Equation (8) will be utilizable only when the entry-state population possesses a very large width (relative to the mean value of spin J).

For massive-transfer and complete-fusion reactions listed in Table II, calculated values of $f_y^2\sigma_M^2/\sigma_J^2$ are indicated in Fig. 10. It is clearly seen that in the case of massive transfer the width of the J distribution (relative to $\langle J\rangle$) is expected to be significantly smaller than that in the case of complete fusion.

The calculated s_M turned out to be positive in the case of massive transfer, as is shown in Table II, while that for complete fusion was negative. We have examined how s_M changes as a function of the widths of E and J distributions. Figure 11 shows the change of s_M with the relative widths $\Delta E/\langle E\rangle$ and $\Delta J/\langle J\rangle$: A narrow J distribution tends to give a positive s_M, while a broader distribution tends to reduce the value of s_M, even resulting in a negative s_M. A broad E distribution tends to give a positive s_M, while a narrow one tends to reduce the value of s_M, resulting in a negative value at large $\Delta J/\langle J\rangle$. It has also been found that these tendencies are enhanced as $\langle J\rangle$ increases. Since the entry-state population $P(E,J)$, as is shown in Fig. 8, is expected to possess larger ΔE and smaller ΔJ in the case of massive transfer than those in the case of complete fusion, the sign of s_M should be positive. In contrast, it should be negative in the case of complete fusion.

TABLE III. Comparison of critical angular momentum Λ_c for fusion of massive fragment with average J value $\langle J_0\rangle$ deduced from γ multiplicity. Critical angular momentum λ_c for fusion of projectile and target nuclei is also compared with average l value $\langle l_i\rangle$ of incident channel leading to massive transfer. See the text for details.

Reaction	$E_{\rm lab}$ (MeV)	$\langle E_\alpha\rangle$ (MeV)	Λ_c ($\hbar$)	$\langle M\rangle$	$\langle J_x\rangle$ ($\hbar$)	$\langle J_0\rangle$ ($\hbar$)	$\langle l_i\rangle$ ($\hbar$)	λ_c ($\hbar$)
^{154}Sm(^{12}C,α4n)^{158}Dy	85	29	24	12.1	16.2	20	40	39
^{154}Sm(^{12}C,α4n)^{158}Dy	109	46	26	14.7	21.4	25	49	47
^{159}Tb(^{14}N,α3n)^{166}Yb	95	30	24	14.0[a]	20.0	23	42	42
^{159}Tb(^{14}N,α5n)^{164}Yb	115	30	32	14.9[b]	21.8	27	50	50
^{154}Sm(^{16}O,α6n)^{160}Er	153	45	42	19.8[c]	31.6	38	63	63

[a]Data are taken from Ref. 18, and corrected for cutoff $2^+\rightarrow 0^+$ transition.
[a]Corrected for cutoff $2^+\rightarrow 0^+$ transition.
[c]Data are taken from Ref. 7.

The sign of skewness is related to the widths of E and J distributions of the entry states, thus eventually to those of ϵ and λ distributions of the initial compound system, but it does not necessarily reflect the asymmetry of the J (or λ) distribution.

V. DISCUSSION

We have studied γ-ray multiplicity distributions in detail for the reactions ^{159}Tb(^{14}N,αxn)$^{169-x}$Yb at 115 MeV and ^{154}Sm(^{12}C,αxn)$^{162-x}$Dy at 85 and 109 MeV. Characteristic features of these massive-transfer reactions ($x < 5$) are as follows:

(1) The average γ-ray multiplicity $\langle M \rangle$ is independent of yrast spin;

(2) $\langle M \rangle$ decreases monotonically with increasing α-particle energy ($E_\alpha \gtrsim 30$ MeV);

(3) The standard deviation σ_M tends to be constant, independent of yrast spin;

(4) The sign of skewness s_M tends to be positive.

In the following we shall show that these features are not characteristic of fusion-evaporation residues.

A. Average γ-ray multiplicity $\langle M \rangle$

Characteristic (1) is obviously related to the lack of sidefeeding which has been noted in experiments determining the intensity of yrast γ rays.[2-4,8] As seen from Figs. 2–4, reactions of this type are ^{159}Tb(^{14}N,αxn)$^{169-x}$Yb with $x=3$, 4, and 5 at 115 MeV; ^{154}Sm(^{12}C,α4n)^{158}Dy at 85 MeV; and ^{154}Sm(^{12}C,αxn)$^{162-x}$Dy with $x=4$ and 5 at 109 MeV. The constancy of $\langle M \rangle$ against yrast spins was also reported by Hageman *et al.*[6] for ^{152}Sm(^{12}C,α4n)^{156}Dy at 95 MeV and by Yamada *et al.*[9] for ^{164}Sm(^{14}N,p9n)^{168}Er at 165 MeV. In their study of preequilibrium effects in fusion of ^{12}C and ^{158}Gd, Sarantites *et al.*[30] noted that $\langle M \rangle$ appeared to be the same for all levels in a given product, and they also reported this tendency for evaporation residues formed in bombardments of ^{150}Nd by ^{20}Ne.[23]

For evaporation residues produced via complete fusion, $\langle M \rangle$ is known to increase with increasing yrast spin.[25,31-35] In the present study, as is shown in Fig. 6, $\langle M \rangle$ increases with yrast spin for slow α-particle emission characteristic of fusion evaporation. When the number of neutrons emitted from the amalgamated system of target and projectile nuclei is large, $\langle M \rangle$ tends to increase somewhat with yrast spin as seen in Figs. 2(a) and 4(a). Alpha particles emitted in these cases are mainly low-energy ones whose most probable energy is at about the Coulomb barrier: ^{159}Tb(^{14}N,α6n)^{163}Yb at 115 MeV and ^{154}Sm(^{12}C,α6n)^{156}Dy at 109 MeV are considered to be complete-fusion reactions unlike other reactions emitting fewer neutrons.

The second feature is not expected for the evaporation residues. As was pointed out in Ref. 18, $\langle M \rangle$ appears independent of E_α in the case of slow α-particle emission near the Coulomb barrier: The $\langle M \rangle$ value is seen to be constant in this region. When the gating α particles are chosen from the high energy part of the α spectrum, it is seen that $\langle M \rangle$ decreases with increasing E_α. If an inclusive $\langle M \rangle$ value is measured for a given reaction system instead of $\langle M \rangle$ for individual exit channels, $\langle M \rangle$ will decrease with increasing E_α as is apparent from Fig. 7. This was observed in Ref. 7.

One concludes that fast α particles are emitted before the target and projectile fuse.

B. Standard deviation σ_M

The present statistical model calculation shows that σ_M in the case of massive transfer should be smaller than that in the case of complete fusion. Experimentally, however, we were not able to demonstrate this clearly in the present study. It is not straightforward to extract information on the width of angular momentum distribution from the experimental value of σ_M. As was suggested by Hageman *et al.*,[6] there is an instrumental width inherent in the experimental σ_M to the extent of 30% of $\langle M \rangle$. Furthermore the experimental method requires that multiplicity data be taken for a range of α energies; this inevitably broadens the multiplicity distributions.[11] Hillis *et al.*[36] also pointed out that the measured width σ_M was larger than the predicted width. However, we have noticed a following remarkable difference in the systematic behavior of σ_M as a function of yrast spin.

For the reactions ($x=6$) which are considered to be complete fusion in the above discussion of $\langle M \rangle$, σ_M tends to decrease with increasing yrast spin up to a certain spin value. [See Figs. 2(a), and probably 4(a).] This behavior of σ_M was actually seen in the previous studies of γ-ray multiplicity distributions for the residual nuclei produced by complete fusion.[6,25,31,33-35] On the other hand, the fact [characteristic (3)] that σ_M tends to be constant independent of yrast spin is considered as an indication that the residual nucleus is produced by incomplete fusion, i.e., an attribute of massive transfer. The present statistical model calculation is consistent with this observation.

C. Skewness s_M

Experimental data reported so far[22,31] and statistical calculations[25,35] show that s_M should be negative in the case of complete fusion. (Sarantites *et al.* reported negative skewness in their study of evaporation residues,[23,30] but their result on $\langle M \rangle$ is rather for incomplete fusion as mentioned in Sec. V A. This suggests that complete and incomplete fusion processes were competing in their reactions.) In the present study, although the statistical uncertainty is large, it is noted that the most probable value of s_M tends to be negative for such a process as the α6n channel, which is considered to be complete fusion from the behavior of $\langle M \rangle$ and σ_M against yrast spins. [See Table I, Figs. 2(a) and 4(a).]

Since slow α-particle emission is characteristic of the fusion-evaporation process, the sign of s_M is expected to be negative at around the Coulomb barrier in α evaporation if it is measured as a function of E_α. As seen from Fig. 7, the present result seems to be in accordance with this expectation. On the other hand, Fig. 7 suggests that the sign of s_M tends to be positive when fast α particles are emitted. This agrees with the fact that residual nuclei associated mainly with energetic α-particle emission, i.e., αxn ($x=3,4,5$) reaction products yielded positive values

as the most probable s_M. (See Table I, and Figs. 2—4.) Geoffroy *et al.*[7] also noted in their inclusive measurements that s_M tended to be positive in the case of energetic α-particle emission, while to be negative in the case of low-energy α-particle emission.

The statistical model calculation described in Sec. IV shows that the sign of s_M is likely to be negative unless the entry-state angular momenta are restricted to a narrowly limited window or the entry-state excitation energy distribution is very broad. Either of these postulates or both will be realized when the residual nucleus is produced via a direct reaction from which α particles are emitted, since the existence of an angular-momentum window in l space is inferred from the angular-momentum matching condition of the direct reaction to the continuum and the excitation-energy distribution is due to the Q window, which is another kinematical condition inherent in the direct reaction.

In the light of the above argument, the fourth feature that the sign of s_M to be positive is certainly not characteristic of complete fusion and it is an indication that massive transfer is a kind of direct reaction. Several theoretical studies of massive transfer (or incomplete fusion) have been made by assuming a direct interaction.[13—17]

D. Comparison with deep-inelastic and quasielastic processes

We have already pointed out a similarity between massive transfer and quasielastic processes.[19—21] Here we shall describe details of such a comparison.

For the ^{86}Kr+^{144}Sm reaction at 490 MeV, Christensen *et al.*[37] reported that the average γ-ray multiplicity $\langle M \rangle$ was almost constant as a function of Q value in the region of the deep-inelastic process, while it decreased monotonically with Q value in the region of the quasielastic process. Although this reaction system, except for the bombarding energy per nucleon, is very much different from those we have studied, the relation of $\langle M \rangle$ with Q value coincides with the behavior of $\langle M \rangle$ with E_α as presented in Fig. 7. Slow α-particle emission corresponds to an energy-dissipative reaction like the deep-inelastic process, and fast α-particle emission resembles a quasielastic process. With this in mind, the relationship between the sign of s_M and Q value is indeed suggestive: the sign of s_M is positive in the quasielastic region, while negative in the deep-inelastic region.[37] This is the same tendency that we expect for s_M as a function of E_α: the sign of s_M is likely to be positive in the case of fast α-particle emission, while negative in the case of slow α-particle emission. (See Fig. 7.)

The above comparison of the γ-ray multiplicity characteristics strongly suggests that the underlying reaction mechanism of massive transfer is not deep inelastic as frequently argued,[38] but resembles rather a quasielastic process.

E. Information on angular momentum

In Ref. 11 an analysis was made that compared $\langle M \rangle$ with the angular momentum of various systems such as target plus massive fragment in the entrance channel and the excited compound systems before and after neutron emission. A more detailed discussion of this kind is presented here.

The compound system formed by the massive transfer, i.e., a massive fragment plus target, usually emits several neutrons before γ deexcitation. The average angular momentum $\langle J_0 \rangle$ of the system at its beginning will be given by $\langle J_0 \rangle = \langle J_X \rangle + \Delta J$, where $\langle J_X \rangle$ is the average spin of the entry-state population, and ΔJ is the angular momentum carried away by neutrons.

In order to convert $\langle M \rangle$ to $\langle J_X \rangle$, we assumed the relation $\langle J_X \rangle = 2\{\langle M \rangle - 4\}$, which is commonly adopted for statistical treatment of γ deexcitation.[33] (Instead of this relationship, there may be somewhat elaborated formulas to convert $\langle M \rangle$ to $\langle J_X \rangle$. Those, however, would not change the result by more than 10% of $\langle J_X \rangle$, i.e., about $2\hbar$ in the present case.) We also assumed that ΔJ per neutron is about $1\hbar$. The typical results of this analysis are presented in Table III.

To estimate the average orbital angular momentum $\langle l_i \rangle$ in the incident channel, we use the reaction kinematics given by Siemens *et al.*[39] for heavy-ion transfer reactions, which is generally believed to be valid for description of the optimal condition for a transfer or breakup process. From the recoil formula[39] that relates relative velocities just before and after the transfer of mass m_X, we have

$$V_{Bb} = \left[\frac{m_A}{m_X + m_A} \right] V_{Aa} \tag{9}$$

for the system $a + A \rightarrow b + B$, $B = X + A$, where b is the spectator particle, and X is the massive fragment. For simplicity we neglect inelastic excitation in both the incoming and outgoing channels. In the systems listed in Table III, $m_A \gg m_X$, so that $V_{Bb} \approx V_{Aa}$. Then the orbital angular momentum of the emitted particle b in the outgoing channel is given by

$$l_b = \frac{\mu_{Bb}}{\mu_{Aa}} \frac{R_f}{R_i} l_i \ , \tag{10}$$

and the orbital angular momentum of the massive fragment X in the $X + A$ system is given by

$$l_X = \frac{\mu_{AX}}{\mu_{Aa}} \frac{R_X}{R_i} l_i \ , \tag{11}$$

where μ denotes a reduced mass, R_i and R_f are the distances between a and A, and between b and B, respectively, and R_X the distance between X and A; l_i is the orbital angular momentum of the projectile a in the $a + A$ system.

If the massive transfer takes place in the reaction plane defined by $\mathbf{k}_a \times \mathbf{k}_b$, we have $l_i = l_b + l_X$, and $\langle l_i \rangle$ can be approximated by $\langle l_i \rangle \approx l_i$ in terms of the classical kinematics. The value of l_X is estimated experimentally from the $\langle M \rangle$ value because l_X should be equal to the average angular momentum transferred to the compound system B, i.e., $l_X \approx \langle J_0 \rangle$.

We shall test this classical model, provided that massive transfer takes place around the critical distance R_c for

fusion[28] of the $a+A$ system, i.e., $R_i=R_c$ and $l_i=\lambda_c$, and that the spectator a particle is emitted at R_a^{int} the strong absorption radius[40]

$$R_a^{\text{int}}=1.07(A_a^{1/3}+A_A^{1/3})+3.0\ , \tag{12}$$

i.e., $R_f=R_a^{\text{int}}$. If this condition is reasonable, we have $\langle l_i\rangle\approx l_b+\langle J_0\rangle$ and $\langle l_i\rangle\approx\lambda_c$ where l_b is given by Eq. (10) with $R_i=R_c$ and $R_f=R_a^{\text{int}}$, and $\langle J_0\rangle$ is determined experimentally through $\langle M\rangle$. As is seen in Table III, the constraint $\langle l_i\rangle=\lambda_c$ is well fulfilled.

The value of R_X, which is estimated from Eq. (11) by the substitution $l_X=\langle J_0\rangle$, turns out somewhat smaller than the critical distance for fusion of X and A. In contrast to this, it should be pointed out that setting $R_X=R_i$ is a prerequisite in Wilczynski's sum-rule model.[17]

Since the incoming heavy ion (and its fragments) possesses a de Broglie wave length short enough to be described classically, we can describe schematically the collision process characteristic of massive transfer on the basis of the above argument. Figure 12(a) shows the instant of collision leading to massive transfer, indicating the spectator particle b to be emitted at R_a^{int} and the massive fragment to be transferred at R_X. The dotted circle indicates the most probable position for the massive fragment X to be transferred. This presentation may be compared to the statement on massive transfer that is based on the breakup-fusion model:[41] the breakup fusion takes place in the deep peripheral region, which is about 2 fm deeper than the usual peripheral region.

For comparison, in Fig. 12(b) is shown an illustration of the so-called preequilibrium light-particle emission: a light fragment b is at the critical distance for fusion of b and A or could be anywhere within the strong absorption radius R_b^{int}. In this case, the collision time becomes eventually longer than that in the case of Fig. 12(a), and the process should be much more energy dissipative.

The present statistical analysis, especially of the sign of s_M (see Fig. 10), shows that $\Delta J/\langle J\rangle$ should be significantly smaller than that in the case of complete fusion. However, to extract the width ΔJ of spin distribution of the entry-state population from σ_M, extreme care should be taken; otherwise, the experimental width of γ-ray multiplicity distribution (σ_M) is very much likely to result in overestimation of ΔJ.

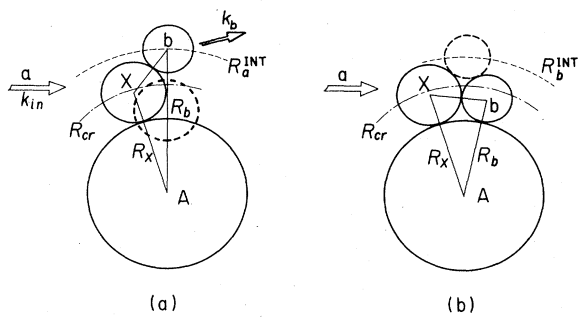

FIG. 12. (a) The instant of massive-transfer reaction $a+A\rightarrow b+(X+A)$: A is the target, b is the spectator particle, and X is the massive fragment. R_b is assumed to be equal to the strong absorption radius R_a^{int} of the $a+A$ system. R_c and R_X indicate critical distances of the $a+A$ and $X+A$ systems, respectively, where the critical angular momenta are defined. The dotted circle indicates the most probable position for X to be transferred. (b) Preequilibrium emission of the light particle b: R_b^{int} is the strong absorption radius of the $b+A$ system, and R_b the critical distance of the same system.

VI. CONCLUSION

We measured γ-ray multiplicity distributions associated with massive transfer and extracted their first three central moments.

The results of a statistical model calculation are generally consistent with the experimental results except for the second moment (variance). The model calculation gives a smaller value of σ_M than the experimental one. At least two experimental factors are involved. Instrumental resolution[6] is one factor and the other results from the spread E_α in analyzing data.[11] Care should be taken to extract the spin width of the entry-state distribution from experimental σ_M. However, the sign of the third moment, i.e., skewness s_M gives information on the width of the excitation-energy and angular momentum distributions. For massive transfer s_M appears to be positive, indicating that the relative width $\Delta J/\langle J\rangle$ is smaller than that for complete fusion. This suggests that there is an l window in the entrance channel of massive-transfer reactions. This conclusion is consistent with the conjecture that was made in interpreting the lack of sidefeeding to low spins.[2–4,8] In addition, the positive value of s_M in massive transfer implies that $\Delta E/\langle E\rangle$ is larger than that for complete fusion, as expected since in massive transfer a spectator particle is emitted with a range of energy, i.e., there is a Q window.

In view of the systematic behavior of $\langle M\rangle$, σ_M, and s_M, massive transfer appears to be a quasielastic process rather than a deep-inelastic one. This result is consistent with the breakup-fusion model,[14] in which the direct breakup of the projectile a into $b+X$ takes place first in the peripheral region and is followed by fusion of the fragment nucleus X and the target nucleus A.

The question of the extent to which angular momentum is localized in massive transfer is a very important one not only from the viewpoint of reaction mechanism but also from the viewpoint of spectroscopy.[11,42] Such localization of angular momentum, however, is still to be proven experimentally. It would be interesting to systematically and precisely measure how the localized l window changes as a function of E_α.

ACKNOWLEDGMENTS

Authors are gratefully indebted to Prof. T. Udagawa, Prof. T. Tamura, and Prof. T. Kishimoto for enlightening discussion. One of the authors (T.I.) expresses his thanks for the kind hospitality extended to him during his stay at the Cyclotron Institute, Texas A&M University. This research was supported in part by the U.S. Department of Energy and the Robert A. Welch Foundation.

*Present address: Westinghouse Electric Corporation, Bettis Atomic Power Laboratory, West Mifflin, PA 15122.
†Present address: Bell Laboratories, Murray Hill, NJ 07974.
‡Present address: Department of Physics, University of Notre Dame, Notre Dame, IN 46556.
§Present address: College of Science, Oregon State University, Corvallis, OR 97331.

[1]H. C. Britt and A. R. Quinton, Phys. Rev. **124**, 877 (1961).
[2]T. Inamura, M. Ishihara, T. Fukuda, T. Shimoda, and K. Hiruta, Phys. Lett. **68B**, 51 (1977); *Lecture Notes in Physics* (Springer, Berlin, 1979), Vol. 29, p. 476, where the revised width of the angular momentum distribution of the entry states was presented as FWHM$=6.6\hbar\pm1.1\hbar$.
[3]D. R. Zolnowski, H. Yamada, S. E. Cala, A. C. Kahler, and T. T. Sugihara, Phys. Rev. Lett. **41**, 92 (1978).
[4]H. Yamada, D. R. Zolnowski, S. E. Cala, A. C. Kahler, J. Pierce, and T. T. Sugihara, Phys. Rev. Lett. **43**, 605 (1979).
[5]K. Siwek-Wilczynska, E. H. du Marchie van Voorthuysen, J. van Popta, R. H. Siemssen, and J. Wilczynski, Phys. Rev. Lett. **42**, 1599 (1979).
[6]D. C. J. M. Hageman, R. V. F. Janssens, J. Lukasiak, W. J. Ockels, Z. Sujkowski, and M. J. A. de Voigt, Phys. Scr. **24**, 145 (1981).
[7]K. A. Geoffroy, D. G. Sarantites, M. L. Halbert, D. C. Hensley, R. A. Dayras, and J. H. Baker, Phys. Rev. Lett. **43**, 1303 (1979).
[8]J. H. Baker, J. R. Beene, M. L. Halbert, D. C. Hensley, M. Jaaskelainen, D. G. Sarantites, and R. Woodward, Phys. Rev. Lett. **45**, 424 (1980).
[9]H. Yamada, C. F. Maguire, J. H. Hamilton, A. V. Ramayya, D. C. Hensley, M. L. Halbert, R. L. Robinson, F. E. Bertrand, and R. Woodward, Phys. Rev. C **24**, 2565 (1981).
[10]H. Tricoire, C. Gerschel, N. Perrin, H. Sergolle, L. Volentin, D. Bachellier, H. Doubre, J. Gizon, Z. Phys. A **306**, 127 (1982).
[11]T. T. Sugihara, Proceedings of Nobel Symposium 50 on Nuclei at Very High Spin, Sven Gösta Nilsson in Memoriam, edited by G. Leander and H. Ryde, Örenäs, Sweden, 1980; Phys. Scr. **24**, 108 (1981).
[12]M. Lefort, Rep. Prog. Phys. **39**, 9 (1976); Phys. Scr. **10A**, 94 (1974).
[13]T. Kishimoto and K.-I. Kubo, Argonne National Laboratory Report ANL/PHY-79-4, 1979, p. 535.
[14]T. Udagawa and T. Tamura, Phys. Rev. Lett. **45**, 1311 (1980); Phys. Rev. C **24**, 1348 (1981).
[15]V. E. Bunakov, V. I. Zagrebaev, and A. A. Kolozhvary, Izv. Akad. Nauk SSSR Ser. Fiz. **44**, 2331 (1980).
[16]J. R. Wu and I. Y. Lee, Phys. Rev. Lett. **45**, 8 (1980).
[17]J. Wilczynski, K. Siwek-Wilczynska, J. van Driel, S. Gonggrijp, D. C. J. M. Hageman, R. V. F. Janssens, J. Lukasiak, and R. H. Siemssen, Phys. Rev. Lett. **45**, 606 (1980); Nucl. Phys. **A373**, 109 (1982).
[18]T. Inamura, T. Kojima, T. Nomura, T. Sugitate, and H. Utsunomiya, Phys. Lett. **84B**, 71 (1979).
[19]T. Inamura and M. Wakai, J. Phys. Soc. Jpn. **51**, 1 (1982).
[20]T. Inamura, *Proceedings of the International School-Seminar on Heavy-Ion Physics, Alushta, USSR, 1983* (Joint Institute of Nuclear Research, Dubna, 1983), p. 298.
[21]T. Inamura, A. C. Kahler, Z. R. Zolnowski, U. Garg, and T. T. Sugihara, *Proceedings of the International Conference on Nuclear Physics, Florence, 1983* (Tipografia Compositori, Bologna, Italy, 1983).
[22]W. J. Ockels, Z. Phys. A **286**, 181 (1978).
[23]D. G. Sarantites, J. H. Baker, M. L. Halbert, D. C. Hensley, R. A. Dayras, E. Eichler, N. R. Johnson, and S. A. Gronemeyer, Phys. Rev. C **14**, 2138 (1976).
[24]Z. Sujikowski and S. Y. van der Werf, Nucl. Instrum. Methods **171**, 445 (1980).
[25]M. Wakai and A. Faessler, Nucl. Phys. **A307**, 349 (1978).
[26]J. Gilat and J. R. Grover, Phys. Rev. C **3**, 734 (1971); J. Gilat, Brookhaven National Laboratory Report No. BNL 50246, 1970.
[27]D. Sperber, Nuovo Cimento **36**, 1164 (1965); J. Gilat, E. R. Jones III, and J. M. Alexander, Phys. Rev. C **7**, 1973 (1973).
[28]M. Lefort and C. Ngo, Ann. Phys. (N.Y.) **3**, 5 (1978).
[29]E. H. Auerbach, Brookhaven National Laboratory Report No. BNL 6562, 1962.
[30]D. G. Sarantites, L. Westerberg, M. L. Halbert, R. A. Dayras, D. C. Hensley, and J. H. Baker, Phys. Rev. C **18**, 774 (1978).
[31]G. B. Hagemann, R. Broda, B. Herskind, M. Ishihara, S. Ogaza, and H. Ryde, Nucl. Phys. **A245**, 166 (1975).
[32]A. Kerek, J. Kihlgren, Th. Lindblad, C. Pomar, J. Sztarker, W. Walus, O. Skeppstedt, J. Bialkowski, J. Kownacki, Z. Sujkowski, and A. Zglinski, Nucl. Instrum. Methods **150**, 483 (1978).
[33]Q. Andersen, R. Bauer, G. B. Hagemann, M. L. Halbert, B. Herskind, M. Neiman, and H. Oeschler, Nucl. Phys. **A295**, 163 (1978).
[34]M. J. A. de Voigt, W. J. Ockels, Z. Sujkowski, A. Zglinski, and J. Mooibroek, Nucl. Phys. **A323**, 317 (1979).
[35]O. Civitarese, A. Faessler, and M. Wakai, Phys. Lett. **84B**, 404 (1979).
[36]D. L. Hillis, J. D. Garrett, O. Christensen, B. Fernandez, G. B. Hagemann, B. Herskind, B. B. Back, and F. Folkmann, Nucl. Phys. **A325**, 216 (1979).
[37]P. R. Christensen, F. Folkmann, Ole Hansen, O. Nathan, N. Trautner, F. Videbaek, S. Y. van der Werf, H. C. Britt, P. R. Chestnut, H. Freisleben, and F. Puhlhofer, Phys. Rev. Lett. **40**, 1245 (1978).
[38]For instance, V. V. Volkov, *Proceedings of the International School-Seminar on Heavy-Ion Physics, Alushta, USSR, 1983* (Joint Institute of Nuclear Research, Dubna, 1983), p. 310; A. G. Artukh, G. F. Gridnev, M. Gruszecki, W. Karcz, A. N. Mezentsev, V. L. Mikheer, L. Pomorski, A. Popescu, D. G. Popescu, and V. V. Volkov, Z. Phys. A **303**, 41 (1981).
[39]P. J. Siemens, J. P. Bondorf, D. H. E. Gross, and F. Dickmann, Phys. Lett. **36B**, 24 (1971).
[40]J. R. Huizenga, F. R. Birkelund, and W. Johnson, Argonne National Laboratory Report ANL/PHY-76-2, 1976, p. 1.
[41]T. Udagawa, D. Price, and T. Tamura, Phys. Lett. **118B**, 45 (1982).
[42]D. R. Haenni, T. T. Sugihara, R. P. Schmidt, G. Mouchaty, and U. Garg, Phys. Rev. C **25**, 1699 (1982).